Eur. Phys. J. B **26**, 449–453 (2002)
DOI: 10.1140/epjb/e20020113

THE EUROPEAN PHYSICAL JOURNAL B
EDP Sciences

The electronic structure of the doped one-dimensional transition metal oxide $Y_{2-x}Ca_xBaNiO_5$ studied using X-ray absorption

Z. Hu[1], M. Knupfer[1,a], M. Kielwein[1], U.K. Rößler[1], M.S. Golden[1], J. Fink[1], F.M.F. de Groot[2], T. Ito[3], K. Oka[3], and G. Kaindl[4]

[1] Institute for Solid State Research, IFW Dresden, 01171 Dresden, Germany
[2] Department of Inorganic Chemistry, University of Utrecht Sorbonnelaan 16, 3584 CA Utrecht, The Netherlands
[3] Correlated Electron Research Center, AIST, 1-1-1 Higashi, Tsukuba, Ibaraki 305-8562, Japan
[4] Institut für Experimentalphysik, Freie Universität Berlin, Arnimallee 14, 14195 Berlin, Germany

Received 7 January 2002

Abstract. A strong anisotropic distribution of the holes in Ni $3d$ and O $2p$ orbitals is observed in the polarization dependent O $1s$ and Ni $2p_{3/2}$ X-ray absorption spectroscopy of the linear-chain nickelate $Y_{2-x}Ca_xBaNiO_5$ ($x = 0$, 0.05, 0.1, 0.2), which demonstrates the one-dimensional nature of the electronic state in these compounds. The holes introduced by Ca-doping occupy both O $2p$ and Ni $3d$ orbitals along the NiO_5 chains. By comparing the experimental Ni $2p_{3/2}$ absorption spectra of $Y_{2-x}Ca_xBaNiO_5$ to those from charge transfer multiplet calculations we can derive the orbital character of the additional holes to be of ∼60% O$2p$ and ∼40% Ni $3d$.

PACS. 78.70.Dm X-ray absorption spectra – 71.28.+d Narrow-band systems; intermediate-valence solids – 79.60.-i Photoemission and photoelectron spectra

1 Introduction

The fundamental physical properties of the one-dimensional (1D) transition metal oxides have attracted a lot of interest in recent years [1–4]. For instance, the discovery of superconductivity in $Sr_{0.4}Ca_{1.36}Cu_{24}O_{41+\delta}$, which has no CuO_2 plane, but rather a linear chain of CuO_4 plaquettes and a two-leg ladder network, has evoked a series studies of the quasi-1D cuprates [5–8]. A theoretical description can be much easier achieved for 1D systems as compared to their two- or three-dimensional relatives, and thus comprehensive studies of one-dimensional highly correlated systems can help to develop or test different model approaches. One of the fascinating aspects of 1D systems lies in Haldane's conjecture that the behavior of antiferromagnetic (AF) quantum spin chains depends crucially on whether the spin is integer or half-integer [9]. The hole doped 1D system $Y_{2-x}Ca_xBaNiO_5$ discovered recently [10] is an ideal system to explore this conjecture. Neutron scattering data have indicated that unlike 2D transition metal (TM) oxides and 1D cuprates [5–8], Y_2BaNiO_5 is not an antiferromagnet but a compound with a quantum disordered ground state and a Haldane gap [3]. This is consistent with the expectation that a $3d^8$ configuration ($S = 1$) exhibits a gap Δ_m between a collective spin ground state and antiferromagnetic order. Neutron scattering studies of Y_2BaNiO_5 showed that $\Delta_m/J = 0.3 \sim 0.4$ (J being the spin coupling within the chain) [11,12], which is in agreement with the prediction $\Delta_m/J \sim 0.41$ from various calculations [13–17]. Band structure calculations proposed that the doping should inhibit the AF behavior and produce a metallic system [18]. A combined study of polycrystalline $Y_{2-x}Ca_xBaNiO_5$ using photoemission and bremsstrahlung isochromat spectroscopy (BIS) showed that the hole doping only slightly reduces the occupied part of the electronic structure and more pronounced changes are observed for the unoccupied part [19]. The modification of the unoccupied electronic states upon Ca-doping can be probed using polarization-dependent X-ray absorption spectroscopy (XAS) on single crystals. This technique allows to measure the unoccupied states both site and orbital selectively. Previously, O $1s$ and Ni $2p_{3/2}$ XAS spectra of $Y_{2-x}Ca_xBaNiO_5$ were reported for $x = 0.15$ [3]. In this work, we report a more systematic study of $Y_{2-x}Ca_xBaNiO_5$ with $x = 0$, 0.05, 0.1, 0.2 using polarization dependent XAS measurements of O $1s$ and Ni $2p_{3/2}$ core excitations. In addition, we compare experimental results to theoretical simulations which allows to study the distribution of the holes in between the O $2p$ and Ni $3d$ orbitals.

2 Experimental

$Y_{2-x}Ca_xBaNiO_5$ single crystals were grown using the traveling-solvent floating zone technique. $Y_{2-x}Ca_xBaNiO_5$ adopts an orthorhombic crystal structure [20]. As shown in Figure 1, distorted corner-sharing

[a] e-mail: m.knupfer@ifw-dresden.de

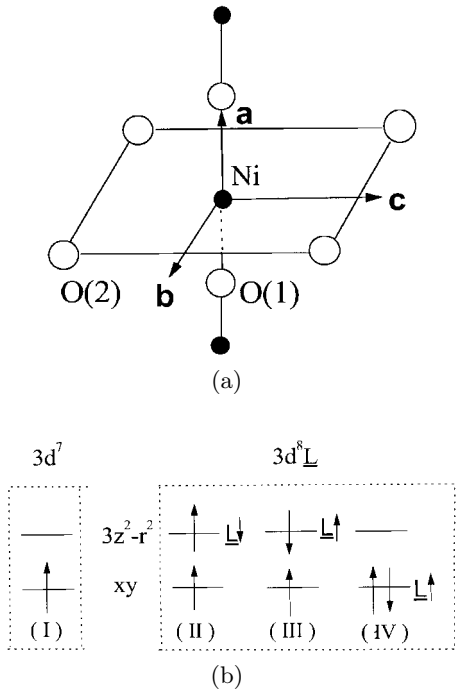

Fig. 1. Schematic view of (a) the NiO_6 clusters which form the NiO_5 chains in Y_2BaNiO_5 and (b) the $3d^7$ and $3d^8\underline{L}$ configurations discussed in the text.

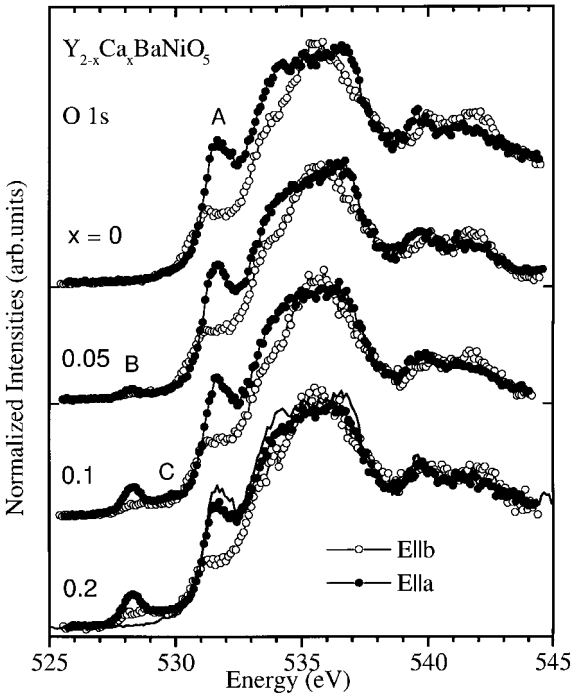

Fig. 2. O 1s X-ray absorption spectra of $Y_{2-x}Ca_xBaNiO_5$ for the light polarization vector **E** parallel to the crystal axes (filled circles **E**||**a**; open circles **E**||**b**). At the bottom the spectrum for **E**||**a** and $x = 0$ is shown again as solid line for comparison.

NiO_6 octahedra form 1D chains along the crystallographic **a**-axis of this system. The Ni-O-Ni angle is 180° and the Ni-O(1) and Ni-O(2) bond lengths are 1.88 Å and 2.18 Å, respectively. The octahedra are slightly squeezed in **b**-direction as compared to the **c**-direction, *i.e.* the local symmetry of Ni is lowered to D_{2h}. Samples have flat **ac** and **ab** surfaces of 3×3 mm^2 size. The XAS experiments were carried out in the non-surface-sensitive fluorescence yield detection mode using linearly polarized light with a normal incidence of the synchrotron radiation from the SX700-II monochromator at BESSY I. The energy resolution of the monochromator was set to be 280 meV and 600 meV at the O 1s and Ni-2p thresholds, respectively. The resulting data were normalized at 80 eV above the absorption thresholds. A correction for self-absorption effects was performed according to a procedure described elsewhere [21,22]. In order to ease a direct comparison of our results with those from other Ni-O based compounds we label the relevant O and Ni orbitals with z along the crystallographic **a** direction (*i.e.* along the Ni-O chains) and with x/y perpendicular to this direction.

3 Results and discussions

In Figure 2 we show the O 1s XAS spectra of $Y_{2-x}Ca_xBaNiO_5$ for the light polarization vector **E** parallel to the crystallographic **a** (filled circles) and **b** (open circles) axes. These measurements probe unoccupied electronic states with O $2p_z$ (**E**||a) and O $2p_x$ (**E**||**b**) character. For Y_2BaNiO_5 the energetically lowest lying structure labeled A in Figure 2 is found at 531.7 eV for **E**||a and at 531.4 eV for **E**||**b**. These energies are close to that observed for the corresponding spectral feature of NiO and these structures are thus assigned to O 2p character mixed with the Ni 3d-derived so-called upper Hubbard band (UHB). The shift of this feature to higher energies for **E**||**a** compared to **E**||**b** is attributed to the distortion of the NiO_6 octahedra along the **a** axis which results in difference of on-site energies for the corresponding oxygen sites as predicted by band structure calculations [18]. The larger intensity for **E**||**a** compared to **E**||**b** reflects the stronger covalence between the O 2p and Ni 3d along the **a** chain with a shorter Ni-O(1) distance.

At a low doping level of $x = 0.05$, a weak pre-edge peak B appears at 528.3 eV for **E**||**a** and at 528.4 eV for **E**||**b**, originating from transitions into the Ca-doping induced O 2p hole states. Upon further Ca-doping, the intensity of peak B increases more strongly for **E**||**a**, which clearly indicates that the holes mainly occupy orbitals along the chain direction, thus underlining the 1 D electronic structure of $Y_{2-x}Ca_xBaNiO_5$. At a doping level of $x = 0.1$ a weak feature C is observed at 529.6 eV for **E**||**a**, similar to what has been found for $x = 0.15$ in a previous study [3]. Furthermore, similar spectral features were also observed in $La_{2-x}Sr_xNiO_4$, where a weak structure corresponding to C was more clearly observed for higher Sr doping levels ($\geq$0.4) [23].

Formally, the Ca-doping leads to the formation of trivalent Ni(III) with a $3d^7$ configuration. Magnetic susceptibility measurements indicate the formation of spin $S = 1/2$ sites upon Ca-doping [24]. As the covalence between Ni and O switches on, the Hamiltonian matrix and the ground state of a $3d^n$ system are given by:

$$H = \begin{vmatrix} 0 & T \\ T & \Delta \end{vmatrix} \quad (1)$$

$$\Phi_g = \alpha_0|3d^n\rangle + \beta_0|3d^{n+1}\underline{L}\rangle, \quad (\alpha_0^2 + \beta_0^2) = 1 \quad (2)$$

$$\beta_0/\alpha_0 = \left\{\left(\Delta^2 + 4T^2\right)^{1/2} - \Delta\right\}/2T \quad (3)$$

where $n = 7$ stands for Ni(III) and $\underline{\mathrm{L}}$ denotes a hole in O $2p$ states (for simplicity we neglect $d^{n+m}\underline{L}^m$ configurations with $m \geq 2$). Δ and T in equations (1, 3) are the charge transfer energy between Ni $3d$ and O $2p$ orbitals and the corresponding transfer integral. Thus, the $3d^7$ state is mixed with $3d^8\underline{L}$ configurations and the degree of this covalent mixture is represented by β_0. There are three different possible $|3d^8\underline{L}\rangle$ configurations mixed with $|3d^7\rangle$. These are depicted in Figure 1b. Two of the $|3d^8\underline{L}\rangle$ configurations involve a hybridization of O $2p_z$ orbitals with Ni $3d(3z^2-r^2)$ states denoted as (II) with spin $S = 1$ and (III) with $S = 0$, while the third one consists of a hybrid of Ni $3d(xy)$ with and O $2p_x/2p_y$ states denoted as (IV) with $S = 0$. The two states with O $2p_z$ contributions can be experimentally observed in our set up for **E**||**a**. As a consequence of Hund's rule, the low spin $3d^8$ states (III) have a higher energy and therefore are more weakly populated as compared to the high spin $3d^8$ configuration (II). The theoretical prediction for this energy splitting between the low and high spin Ni $3d^8$ configurations is 1.3 eV [17] which is comparable with the observed separation between peak B and C for **E**||**a** in Figure 2. We thus assign peaks B and C for **E**||**a** to excitations into high and low spin Ni $3d^8$ states, respectively, which are hybridized with O $2p_z$ orbitals pointing along chains in $Y_{2-x}Ca_xBaNiO_5$. The broad pre-edge peak for **E**||**b** consequently originates from the hybridized state resulting between the $3d_{xy}$ and the $O2p_x/O2p_y$ states as shown in Figure 1b(IV). Its excitation energy relative to the corresponding peaks for **E**||**a** is determined by the Hund's rule coupling as well as by the different on-site energies of the O $2p_x/2p_y$ and the O $2p_z$ resulting from different Madelung potentials. The significantly higher spectral weight of the pre-edge features for **E**||**a** demonstrates that the Ni-O hybridization is stronger along the NiO_5 chains than perpendicular to them due to shorter Ni-O bond length along the chains. Finally, at the bottom of Figure 2 we directly compare the spectra for **E**||**a** of the compounds with $x = 0$ (solid line) and $x = 0.2$. It is clearly seen that the spectral weight of peak A is reduced upon doping which is a result of a spectral weight transfer form the UHB (peak A) to the doping induced features B and C. Such a spectral weight transfer is a direct signature of a strongly correlated electron system and has been studied experimentally [25,26] and theoretically [27,28].

Figure 3 shows the Ni-L_3 XAS spectra of $Y_{2-x}Ca_xBaNiO_5$ and $Nd_{0.9}Sr_{1.1}NiO_{4-0.05}$ as a 2D Ni(III) reference compound. The spectral profile of Y_2BaNiO_5 for **E**||**b** (open circles) consists of a dominant peak A at 853 eV and a broad shoulder B at about 2 eV higher energy. The spectral profile for **E**||**c** is very similar to that for **E**||**b** and is not shown here. In contrast to the O $1s$ spectra, the main feature A is less intensive for **E**||**a** than for **E**||**c**. This confirms the above interpretation that there is a larger O $2p$ contribution to the UHB along the **a** axis.

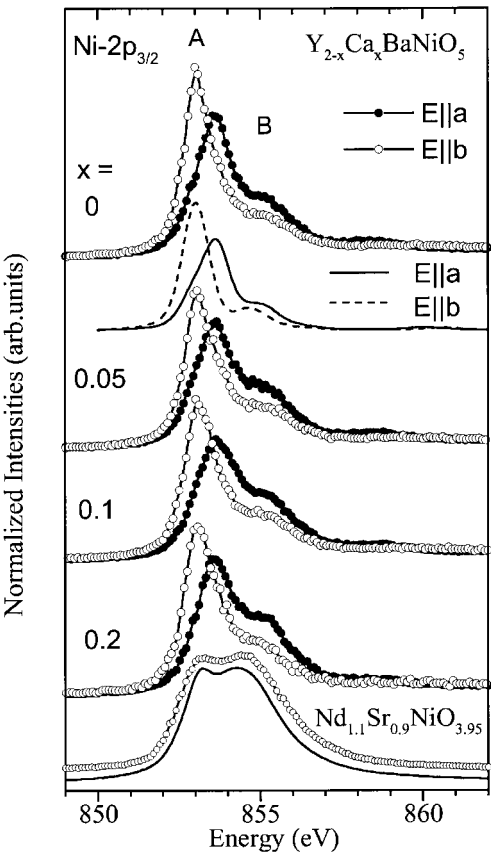

Fig. 3. Ni $2p_{3/2}$ X-ray absorption spectra of $Y_{2-x}Ca_xBaNiO_5$ for the light polarization vector **E** parallel to the crystal axes (filled circles **E**||**a**; open circles **E**||**b**) as well as of $Nd_{0.9}Sr_{1.1}NiO_{4\text{-}0.05}$ as a Ni(III) reference compound. The theoretical curves obtained carrying out charge transfer multiplet calculations are given as solid/dashed lines below the data.

In addition, for **E**||**a** the dominant peak A is shifted by 0.7 eV to higher energy with respect to that for **E**||**b** while the high energy shoulder B appears at the same energy (855 eV) in both cases. Since the spectra for **E**||**a** and **E**||**b** result from transitions from Ni $2p_{3/2}$ to Ni $3d(3z^2 - r^2)$ and $3d(xy)$ states, respectively, the energy shift of peak A of about 0.7 eV is basically a measure for the crystal field splitting between $3d(3z^2 - r^2)$ and $3d(xy)$ states caused by the pseudo-tetragonal distortion of the NiO_6 octahedra in Y_2BaNiO_5. Thus, the tetragonal splitting of the e_g-derived $3d$ states is about half of the octahedral e_g–t_{2g} crystal field splitting (10 Dq) which has been estimated to be 1.3–1.5 eV for the related three-dimensional compound NiO [29,30].

We note that the tetragonal splitting observed here for Y_2BaNiO_5 is much smaller than that previously reported for $La_2NiO_{4-\delta}$ of 1.3 eV [23]. We argue that in the latter case the reported experimental value is overestimated, as it results from the analysis of the Ni $2p_{1/2}$ absorption spectrum where the shoulder strongly changes in intensity as a function of polarization, rendering the analysis of the tetragonal splitting difficult and less conclusive.

Upon Ca-doping the spectral weight of the shoulder B increases more strongly in the case of **E**||**a** compared to **E**||**b**. This again demonstrates that the additional holes in the NiO_5 chains of Y_2BaNiO_5 predominantly occupy orbitals along the chain axis. Generally, this increase of spectral weight at the high energy side upon doping parallels the changes seen in the Ni $2p_{3/2}$ XAS of the compound $Nd_{2-x}Sr_xNiO_{4-\delta}$ with increasing Sr doping, and indicates the transition from a formally divalent to a formally trivalent Ni-O system [31]. To further illustrate this, we have included the Ni $2p_{3/2}$ spectrum of the formally trivalent two dimensional (2D) nickel compound $Nd_{0.9}Sr_{1.1}NiO_{4\text{-}0.05}$. We note that in the latter case, there is no single crystal available. This, however, does not change the conclusions drawn below as $Nd_{0.9}Sr_{1.1}NiO_{4\text{-}0.05}$ contains essentially undistorted NiO_6 octahedra, *i.e.* the XAS spectra are essentially polarization independent. The spectral features of $Nd_{0.9}Sr_{1.1}NiO_{4\text{-}0.05}$ are similar to those observed in an XAS study of other formally trivalent Ni compounds, such as $PrNiO_3$ and $NdNiO_3$ [32]. Figure 3 demonstrates that upon doping, *i.e.* with increase of the valence from Ni(II) to Ni(III), spectral weight is transferred from the lower energy peak A to peak B, which reflects an increase of the effective Ni $2p$ core hole potential due to poorer screening resulting from decrease in the valence electron count. Furthermore, the Ni-$2p_{3/2}$ spectra become broader due to an increase of the O $2p$ admixture in the wave function, since Δ is expected to decreased by as much as 3 eV going from Ni(II) to Ni(III) compounds [31,33]. The polarization dependent Ni $2p_{3/2}$ XAS spectra of undoped Y_2BaNiO_5 can be well reproduced using charge-transfer atomic multiplet calculations applying using (ionic) tetragonal crystal-field values 10 $Dq = 0.8$ eV and $Ds = 0.2$ eV [31,33]. The $3d^9\underline{L}$ state is found to lie 3 eV above the $3d^8$ state in the ground state of a Ni(II) compound, whereby the charge transfer energy Δ is defined here as the energy difference between the energetically lowest $3d^n$ and the lowest $3d^{n+1}\underline{L}$ state. The solid and the dashed curves below the experimental data for Y_2BaNiO_5 and $Nd_{0.9}Sr_{1.1}NiO_{4\text{-}0.05}$ in Figure 3 depict the theoretical results for **E**||**a** and **E**||**b**, respectively. The ground state consists of a mixture of 85% $3d^8$ and 15% $3d^9\underline{L}$ which reflects the predominantly ionic character of the Ni(II) compounds. The theoretical spectrum of the Ni(III) compound is reproduced by decreasing the charge transfer energy from 3 eV for Y_2BaNiO_5 to 0.4 eV for $Nd_{0.9}Sr_{1.1}NiO_{4\text{-}0.05}$. Consequently, the $3d^7$ weight in the ground state of $Nd_{0.9}Sr_{1.1}NiO_{4.0.05}$ was found to be 40%, which is much smaller than 85% $3d^8$ contribution in Y_2BaNiO_5 (Ni[II]) indicating a significant increase of covalence on going from Ni(II) to Ni(III) in agreement with previous studies of other Ni-O materials [31].

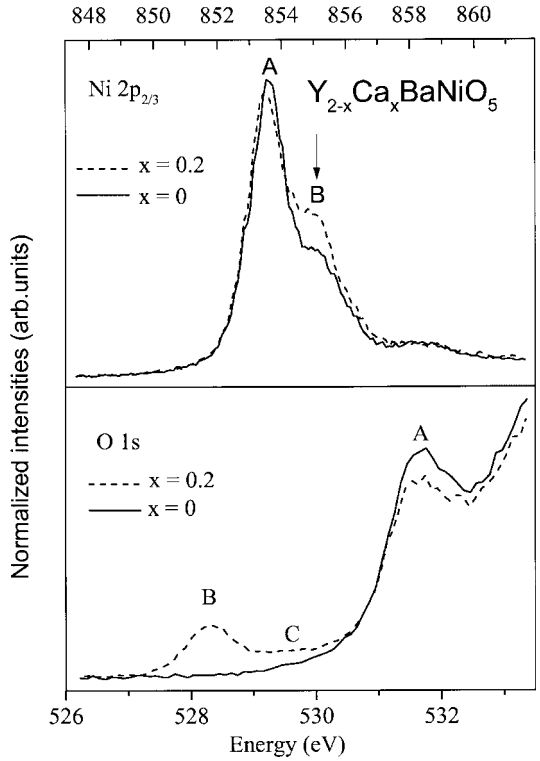

Fig. 4. Comparising the Ni-$2p_{3/2}$ (top) and O $1s$ (bottom) X-ray absorption spectra between doping levels of $x = 0$ and $x = 0.2$ for **E**||**a**.

For a small doping level $x \leq 0.2$, the $3d^7$ weight is certainly smaller than that in the reference compound $Nd_{1.1}Sr_{0.9}NiO_{4\text{-}0.05}$, but one cannot conclude that the doping induced holes have exclusively mainly O $2p$ character. In order to illustrate the distribution of the additional holes between the Ni and O orbitals involved, we show in Figure 4 a comparison of the Ni $2p_{3/2}$ (top of Fig. 4) and the O $1s$ (bottom of Fig. 4) spectra taken at doping levels $x = 0$ and $x = 0.2$ and for **E**||**a**. Going from $x = 0$ to $x = 0.2$, we observe an increase of intensity by 12% and 8% for a sum of the O1s features A, B and C and the Ni $2p_{3/2}$ features A and B, respectively. This would suggest that the doping induced holes have about 40% Ni $3d$ character. A more quantitative analysis of the distribution of the additional holes in the doped compounds based upon theoretical simulation would be intensive, but is beyond the scope of the present paper.

4 Summary

We have presented systematic O $1s$ and Ni $2p_{3/2}$ X-ray absorption spectroscopy studies of the doped one-dimensional transition metal oxide $Y_{2-x}Ca_xBaNiO_5$ ($x =$ 0, 0.05, 0.1, 0.2). Our results demonstrate that the doping induced holes predominantly occupy O $2p$ and Ni $3d$ orbitals that are oriented along the NiO_5 chains in this

compound. This emphasizes the one-dimensional nature of the electronic states in this material. The energy splitting between a high and low spin Ni $3d^8$ configuration could be experimentally determined to be about 1.3 eV in good agreement with theoretical predictions. A comparison of the Ni $2p_{3/2}$ absorption spectra to those from a formally trivalent nickel oxide as well as to cluster calculations showed that the doping induced holes occupy both O $2p$ and Ni $3d$ orbitals, with the ratio for $x = 0.2$ being roughly 2/3.

We acknowledge financial support by Deutsche Forschungsgemeinschaft (SPP1073 [(Fi439/7-1, Fi439/10-1] and SFB 463 "Seltenerd-Übergangsmetallverbindungen: Struktur, Magnetismus und Transport").

References

1. E. Dagotto, T.M. Rice, Science **271**, 618 (1996).
2. N. Motoyama, H. Eisaki, S. Uchida, Phys. Rev. Lett. **76**, 3212 (1996).
3. J.F. DiTusa, S.-W. Cheong, J.-H. Park, G. Aeppli, C. Broholm, C.T. Chen, Phys. Rev. Lett. **73**, 1857 (1994).
4. S.V. Moshkin, S.I. Goloshchapov, O.V. Frank-Kamenetskaya, I.I. Bannova, T.I. Ivanova, T.N. Kaminskaya, M.A. Kuz'mina, M. Yu. Vlasov, Tech. Phys. Lett. **23**, 954 (1997).
5. J. Karpinski, H. Schwer, G.I. Meijer, K. Conder, E.M. Kopnin, C. Rossel, Physica C **274**, 99 (1997).
6. G.I. Meijer, C. Rossel, W. Heinggeler, L. Keller, F. Fauth, J. Karpinski, H. Schwer, E.M. Kopnin, P. Wachter, R.C. Black, J. Diederichs, Phys. Rev. Lett. **58**, 14452 (1998).
7. A. Shengelaya, G.I. Meijer, J. Karpinski, Guo-meng Zhao, H. Schwer, E.M. Kopnin, C. Rossel, H. Keller, Phys. Rev. Lett. **80**, 3626 (1998).
8. I.V. Rozhdestvenskaya, T.I. Ivanova, O.V. Frank-Kamenetskaya, Physica C **311**, 239 (1999).
9. F.D.M. Haldane, Phys. Lett. A **93**, 464 (1983); Phys. Rev. Lett. **50**, 1153 (1983).
10. E. García-Matres, J.L. Martínez, J. Rodríguet-Carvajal, J.A. Alonso, A. Salinas Sánchez, E. Saez-Puche, J. Solid State Chem. **103**, 322 (1993).
11. T. Yokoo, T. Sakaguchi, K. Kakurai, J. Akimitsu, J. Phys. Soc. Jpn **64**, 3651 (1995).
12. T. Sakaguchi, K. Kakurai, T. Yokoo, J. Akimitsu, J. Phys. Soc. Jpn **65**, 3025 (1996).
13. M. Takahashi, Phys. Rev. Lett. **62**, 2313 (1989).
14. S. Liang, Phys. Rev. Lett. **64**, 1597 (1990).
15. S. Yamamoto, Phys. Lett. A **213**, 102 (1996).
16. U. Schollwöck, O. Golinelli, T. Jolicœur, Phys. Rev. B **54**, 4038 (1996).
17. E. Dagotto, J. Riera, A. Sandvik, A. Moreo, Phys. Rev. Lett. **76**, 1731 (1996).
18. L.F. Matteiss, Phys. Rev. B **48**, 4352 (1993).
19. K. Maiti, D.D. Sarma, Phys. Rev. B **58**, 9746 (1998).
20. J. Amador, E. Gutiérrez-Puebla, M.A. Monge, I. Rasines, C. Ruíz-Valero, F. Fernández, R. Sáez-Puche, J.A. Campá, Phys. Rev. B **42**, 7918 (1990).
21. J. Jaklevic, J.A. Kirby, M.P. Klein, A.S. Robertson, Solid State Commun. **23**, 679 (1977).
22. L. Tröger, D. Arvanitis, K. Baberschke, H. Michaelis, U. Grimm, E. Zschech, Phys. Rev. B **46** 3283 (1992).
23. E. Pellegrin, J. Zaanen, H.-J. Lin, G. Meigs, C.T. Chen, G.H. Ho, H. Eisaki, S. Uchida, Phys. Rev. B **53**, 10667 (1996).
24. K. Kojima, A. Keren, L.P. Le, G.M. Luke, B. Nachumi, W.-D. Wu, Y.J. Uemura, K. Kiyono, S. Miyasaka, H. Takagi, S. Uchida, Phys. Rev. Lett. **74**, 3471 (1995).
25. C.T. Chen, F. Sette, Y. Ma, M.S. Hybertsen, E.B. Stechel, W.M.C. Foulkes, M. Schulter, S.-W. Cheong, A.S. Cooper, L.W. Rupp Jr., B. Batlogg, Y.L. Soo, Z.H. Ming, A. Krol, Y.H. Kao, Phys. Rev. Lett. **66**, 104 (1991).
26. J. Fink, N. Nücker, E. Pellegrin, H. Romberg, M. Alexander, M. Knupfer, J. Electron Spectrosc. Relat. Phenom. **66**, 395 (1994).
27. H. Eskes, M.B.J. Meinders, G.A. Sawatzky, Phys. Rev. Lett. **67**, 1035 (1993).
28. M.B.J. Meinders, H. Eskes, G.A. Sawatzky, Phys. Rev. B **48**, 3916 (1993).
29. G. van der Laan, I.W. Kirkman, J. Phys. Cond. Matt. **4**, 5459 (1990).
30. J. van Elp, H. Eskes, P. Kuiper, G.A. Sawatzky, Phys. Rev. B **45**, 1612 (1992).
31. Z. Hu, M.S. Golden, J. Fink, G. Kaindl, S.A. Warda, D. Reinen, Priya Mahadevan, Phys. Rev. B **61**, 3739 (2000).
32. M. Medarde, A. Fontaine, J.L. García-Muñoz, J. Rodríguuez-Carvajal, M. de Santis, M. Saccchi, G. Rossi, P. Lacorre, Phys. Rev. B **16**, 14975 (1992).
33. Z. Hu, C. Mazumdar, G. Kaindl, F.M.F. de Groot, S.A. Warda, D. Reinen, Chem. Phys. Lett. **297**, 321 (1998).